Advances in Applied Mathematics and Mechanics
Adv. Appl. Math. Mech., Vol. **2**, No. 6, pp. 763-783

DOI: 10.4208/aamm.09-m0997
December 2010

Numerical Study of Double Diffusive Convection in Partially Heated Vertical Open Ended Cylindrical Annulus

Mani Sankar*

[1] *Department of Mathematics, East Point College of Engineering and Technology, Bangalore-560 049, India*

Received 29 October 2009; Accepted (in revised version) 8 July 2010
Available online 26 August 2010

Abstract. A numerical investigation of laminar natural double diffusive convection in an open ended vertical cylindrical annulus with unheated entry and unheated exit is performed. Both boundary conditions of uniform wall temperature/uniform wall concentration (UWT/UWC) and uniform heat flux/uniform mass flux (UHF/UMF) are considered. Results of dimensionless induced volume rate Q, average Nusselt number $\overline{Nu}$ and Sherwood number $\overline{Sh}$ are obtained for air flow under various buoyancy ratio N, Grashof numbers due to heat and mass transfer Gr_T and Gr_M, Schmidt number Sc and combinations of unheated entry, heated section and unheated exit length. Since the flow under consideration is a boundary layer type, the governing partial differential equations was discretized to a linear system of equations by the use of an implicit finite difference method. The nonlinear convective terms are approximated by second upwind difference method for the numerical stability. The numerical results reveal that the presence of unheated entry and unheated exit severely affects the heat and mass transfer rates. The numerical solutions are found to approach asymptotically the closed form solutions for fully developed flow. Further, the present numerical results are validated with the existing solutions for pure thermal convection and are found to be in good agreement.

AMS subject classifications: 65L12, 76D05, 80A20

Key words: Discrete heating, cylindrical annulus, upwind difference, doubles diffusive convection, buoyancy ratio.

1 Introduction

Many practical systems involve convective heat and mass transfer in fluids in heated, vertical, open-ended channels like circular tubes, parallel plates and annular cavities.

*Corresponding author.
Email: manisankarir@yahoo.com (M. Sankar)

Noticeable examples include the chemical distillatory processes, design of heat exchangers, channel type solar energy collectors and thermo-protection systems. Hence, the characteristics of natural convection heat and mass transfer are relatively important in the above mentioned applications. Among the above geometries, vertical open-ended cylindrical annulus whose side walls are at different temperatures and concentrations is the most general cavity since it includes the circular tubes and parallel plates as its limiting geometries. Such systems are of practical importance in the field of double pipe arrangements, particularly the fuel elements of nuclear reactors during the shut-off periods. Also the present day technological and engineering environment and style of living in metropolis are demanding hazard-free and safe electrical power supply equipments. In addition, to provide a cleaner and risk-free environment, considerable emphasis has been given on the pollution free equipments.

The natural convection heat transfer in vertical open annular duct flows induced by the thermal buoyancy alone has been investigated in great detail in the literature. El-Shaarawi and Sarhan [1] presented numerical results for the laminar natural convection heat transfer in an open ended vertical concentric annulus of radius ratio 0.5 with one wall being isothermal and other wall being adiabatic. Coney and El-Shaarawi [2] used the finite difference analysis for the incompressible laminar convective flow in concentric annuli with simultaneous development of hydrodynamic and thermal boundary layers and found that the rate of heat transfer for the case of isothermal inner wall and adiabatic outer wall is higher than that of the case of isothermal outer wall and adiabatic inner wall. Later, El-Shaarawi and Sarhan [3] developed a finite difference scheme for the laminar free convective flow in an open ended vertical concentric annuli with rotating inner wall and concluded that heating the inner cylinder has always stabilising effect while heating the outer cylinder has either destabilising or stabilising effect, depending on the nature of the rotation. Numerical investigation of laminar mixed convection in a vertical annulus was studied by Hashimoto et al. [4]. Al-Nimar [5] obtained an analytical solution for transient laminar fully developed free convection in vertical concentric annulus corresponding to four thermal boundary conditions. Recently, natural convection heat and mass transfer in vertical concentric annuli with film evaporation and condensation is performed numerically by Yan and Lin [6].

Natural convection due to heat and/or mass transfer in vertical parallel plates is also studied in detail. A numerical solution based on a finite difference scheme was first obtained by Bodia and Osterle [7] for the development of free convection heat transfer between heated vertical parallel plates. Their finite difference calculations show that the development height is rather significant and for most situations the assumption of fully developed flow is not valid. Yan and Lin [8] considered the effect of the discrete heating on the vertical parallel channel flows driven by buoyancy force and found that the rate of heat transfer is more for continuous heating. The effect of unheated entry and unheated exit section on the natural convection of air flow in a vertical parallel plate channel is numerically investigated by Lee [9]. He considered the uniform heat flux (UHF) and uniform wall temperature (UWT) thermal bound-

ary conditions at the aide walls and found that the heat transfer characteristics are significantly altered with the unheated entry and unheated exit for the case of UHF condition. Nelson and wood [10] analysed the combined heat and mass transfer in vertical plates for both uniform wall temperature and uniform wall heat flux. A numerical study for combined effects of thermal and species diffusion along a vertical cylinder was proposed by Chen and Yeh [11]. Later, Lee [12] presented a combined numerical and theoretical investigation of laminar natural convection heat and mass transfer in open vertical parallel plates with discrete heating for both the boundary conditions of UWT/UWC and UHF/UMF. Also, Lee [13] studied the fully developed double-diffusive natural convection in a partially heated pipe. Cheng [14] examined the fully developed natural convection heat and mass transfer in a vertical annular cavity filled with porous media. He found that the volume flow rate can be increased by increasing the Darcy number or inner radius-gap ratio or the buoyancy ratio. Recently, natural convection from a uniformly heated vertical circular pipe is investigated by Mohammed and Salman [15] for different entry restriction configurations of the pipe.

The studies reviewed above deal with uniform or discrete heating of vertical parallel plates or uniform heating of vertical cylindrical annuli for single diffusive or double diffusive convection. Regardless of its importance in engineering applications, the natural convection heat and mass transfer in vertical open annular duct with discrete heating conditions at the surface forming the annular duct has not been studied in the literature. The effect of unheated portion at the entry and exit of an annular duct will alter the flow behaviour and heat transfer characteristics, which is encountered in many electronic cooling devices and other thermal systems. The purpose of the present numerical study is to investigate the double diffusive convection through a vertical annulus for different Grashof numbers and other dimensionless parameters of the problem with the objective of understanding the effect of discrete heating. The governing equations of the problem are simplified by Prandtl boundary layer approximation. However, the difficulty in finding the analytical solution to these equations comes from the non-linearity of convective terms and also due to their coupled nature. Also, since the flow under consideration is a boundary layer type, a fully implicit numerical scheme has been used to transform the governing equations into finite difference equations. The solution of these finite difference equations are marched in the downstream direction using a Gauss Jordan method and Thomas algorithm.

2 Mathematical formulation

The geometry of the problem under consideration, which is a vertical annulus of finite length l and width $2b$ open at both ends with the inner and outer radii r_i and r_0 respectively, and the coordinate system used are as shown in Fig. 1. Let the inner and outer wall of the annulus be insulated in the bottom and top, while the remaining portion is subjected to uniform temperature (or heat flux) and uniform concentration (or mass flux). Further, the heated portions at top (L_1) and bottom (L_3) are assumed be of same

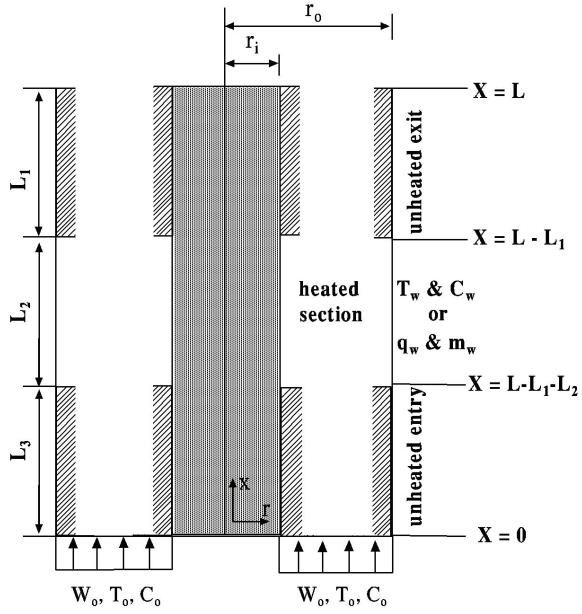

Figure 1: Physical domain, coordinate system and boundary conditions.

lengths. The effect of unheated entry or exit is studied through the non-dimensional parameter, namely, the heater length ratio E. The heat added to the annulus boundaries produces an upward double diffusive natural convective flow in the annular gap between the two cylindrical walls. It is assumed that the fluid enters the bottom of the annulus with a flat velocity profile at a value equal to the mean axial velocity (w_0) in the annular gap and with a uniform temperature and concentration profile at a value equal to the ambient temperature θ_0 and concentration S_0. The fluid is assumed to have constant physical properties but obeys the Boussinesq approximation and the surface normal velocity is ignored due to the small temperature and concentration differences. Also we assume that the flow is steady, axisymmetric and without internal heat generation and viscous dissipation. Under the above assumption the equations of conservation of mass, momentum and energy are as follows (Coney and El-Shaarawi [2]):

$$\frac{\partial}{\partial r}(ur)+\frac{\partial}{\partial x}(wr)=0, \tag{2.1a}$$

$$\frac{1}{r}\frac{\partial}{\partial r}(ru^2)+\frac{\partial}{\partial x}(wu)=-\frac{1}{\rho_0}\frac{\partial p}{\partial r}+\nu\Big[\nabla_1^2 u-\frac{u}{r^2}\Big], \tag{2.1b}$$

$$\frac{1}{r}\frac{\partial}{\partial r}(ruw)+\frac{\partial}{\partial x}(w^2)=-\frac{1}{\rho_0}\frac{\partial p}{\partial x}+\nu\nabla_1^2 w-g\beta_T(\theta-\theta_c)+g\beta_S(S-S_c), \tag{2.1c}$$

$$\frac{1}{r}\frac{\partial}{\partial r}(ru\theta)+\frac{\partial}{\partial x}(w\theta)=\alpha\nabla_1^2\theta, \tag{2.1d}$$

$$\frac{1}{r}\frac{\partial}{\partial r}(ruS)+\frac{\partial}{\partial x}(wS)=D\nabla_1^2 S, \tag{2.1e}$$

where β_T and β_S is the thermal and solutal expansion coefficient, θ_w is the isothermal

wall temperature and (u,w) are the velocity components in (r,x) directions. Also

$$\nabla_1^2 = \frac{\partial^2}{\partial r^2} + \frac{1}{r}\frac{\partial}{\partial r} + \frac{\partial^2}{\partial x^2}.$$

Here the effect of temperature on fluid is unstable and that of concentration is stable.

Further, if we apply the usual Prandtl boundary layer assumptions and check the order of magnitude of each term of the Eqs. (2.1b) and (2.1c), the momentum equations reduce to the following simplified equation:

$$\begin{aligned}&\frac{1}{r}\frac{\partial}{\partial r}(ruw) + \frac{\partial}{\partial x}(w^2)\\ &= -\frac{1}{\rho_0}\frac{\partial p}{\partial x} + \nu\Big(\frac{\partial^2 w}{\partial r^2} + \frac{1}{r}\frac{\partial w}{\partial r}\Big) + g\beta_T(\theta-\theta_c) + g\beta_S(S-S_c).\end{aligned} \tag{2.2}$$

Also, if we neglect the axial diffusion term in the energy and species equations compared to the radial diffusion term, then the Eqs. (2.1d) and (2.1e) reduces to

$$\frac{1}{r}\frac{\partial}{\partial r}(ru\theta) + \frac{\partial}{\partial x}(w\theta) = \alpha\Big(\frac{\partial^2\theta}{\partial r^2} + \frac{1}{r}\frac{\partial\theta}{\partial r}\Big), \tag{2.3a}$$

$$\frac{1}{r}\frac{\partial}{\partial r}(ruS) + \frac{\partial}{\partial x}(wS) = \alpha\Big(\frac{\partial^2 S}{\partial r^2} + \frac{1}{r}\frac{\partial S}{\partial r}\Big). \tag{2.3b}$$

The principal of continuity can be expressed in the following integral form (Coney and El-Shaarawi [2] and Lewis et al. [16])

$$q = \pi(r_o^2 - r_i^2)w_0 = \int_{r_i}^{r_o} 2\pi r w dr. \tag{2.4}$$

In the above integral continuity equation, it has been assumed that the flow enters the annulus with a flat velocity profile at a value equal to the mean axial velocity in the annular gap.

The boundary conditions, in dimensional form, are

$$\begin{array}{lll}
x=0: & u=0,\ w=w_0,\ S=\theta=0 \text{ and } p* = -\dfrac{\rho_0 w_0^2}{2}, & \\
r=r_i: & u=w=0,\ \theta=\theta_w \text{ and } S=S_w, \text{ for UWT/UWC} & \Big\}\text{for heated region}\\
r=r_o: & \dfrac{\partial\theta}{\partial r}=\dfrac{q_w}{k} \text{ and } \dfrac{\partial S}{\partial r}=\dfrac{m_w}{D}, \text{ for UHF/UMF} & \Big\}\\
 & \dfrac{\partial\theta}{\partial r}=\dfrac{\partial S}{\partial r}=0, & \text{for unheated region}\\
x=l: & p*=0. &
\end{array}$$

Applying Bernoulli's equation at the entrance cross section and noting that the origin of the coordinate system is located at the inlet shows that the pressure, p^*, at entry is equal to $-\rho_0 w_0^2/2$ (El-Shaarawi and Sarhan [3]). Assuming that the streamlines in the emerging flow are parallel, the pressure at the channel exit could be specified as zero.

This assumption is in good agreement with all the previous theoretical studies and is equivalent to assuming that the flow from the outlet section is a free jet.

Introducing the following dimensionless variables,

$$U=\frac{ur_0}{v},\qquad W=\frac{wr_0^2}{lGrv},\qquad T=\frac{\theta-\theta_0}{\Delta\theta},\qquad C=\frac{S-S_0}{\Delta S},$$
$$R=\frac{r}{r_0},\qquad X=\frac{x}{lGr},\qquad P=\frac{p*r_0^4}{\rho_0 l^2 v^2 Gr^2},\qquad \lambda=\frac{r_i}{r_0},$$
$$E=\frac{L_1}{L_2},\qquad N=\frac{\beta_C\Delta S}{\beta_T\Delta\theta},\qquad Q=\frac{q}{\pi lvGr},$$

where

$$\Delta\theta=\theta_w-\theta_0,\qquad \Delta S=S_w-S_0,$$

for UWT/UWC, and

$$\Delta\theta=q_w\frac{D_h}{2k},\qquad \Delta S=m_w\frac{D_h}{2k},$$

for UHF/UMF,

$$D_h=r_0-r_i,$$

L_1 and L_2 are lengths of heated and unheated regions. $Gr_T{=}g\beta_T D_h^4\Delta\theta/lv^2$ and $Gr_M{=}g\beta_C D_h^4\Delta S/lv^2$, Grashof numbers for heat and mass transfer, $\mathrm{Pr}{=}v/\alpha$ and $Sc{=}v/D$, Prandtl and Schmidt numbers.

Eqs. (2.1a), (2.2), (2.3a), (2.3b) and (2.4) can be written in the following dimensionless form:

$$\frac{\partial U}{\partial R}+\frac{\partial W}{\partial X}+\frac{U}{R}=0, \tag{2.5a}$$
$$U\frac{\partial W}{\partial R}+W\frac{\partial W}{\partial X}=-\frac{\partial P}{\partial X}+\frac{\partial^2 W}{\partial R^2}+\frac{1}{R}\frac{\partial W}{\partial R}+\Big[\frac{T+NC}{16(\lambda-1)^4}\Big], \tag{2.5b}$$
$$U\frac{\partial T}{\partial R}+W\frac{\partial T}{\partial X}=\frac{1}{\mathrm{Pr}}\Big[\frac{\partial^2 T}{\partial R^2}+\frac{1}{R}\frac{\partial T}{\partial R}\Big], \tag{2.5c}$$
$$U\frac{\partial C}{\partial R}+W\frac{\partial C}{\partial X}=\frac{1}{Sc}\Big[\frac{\partial^2 C}{\partial R^2}+\frac{1}{R}\frac{\partial C}{\partial R}\Big], \tag{2.5d}$$
$$Q=(\lambda-1)^2W_0=2\int_\lambda^1 RW\,dR. \tag{2.5e}$$

The dimensionless boundary conditions are

$$\begin{aligned}
&X=0: \quad U=0,\ W=W_0,\ C=T=0 \text{ and } P=-\frac{W_0^2}{2},\\
&R=\lambda: \quad U=W=0,\ T=1 \text{ and } C=1 \text{ for UWT/UWC}\\
&R=1: \quad \frac{\partial T}{\partial R}=\frac{1}{1-\lambda} \text{ and } \frac{\partial C}{\partial R}=\frac{1}{1-\lambda} \text{ for UHF/UMF}\Big\}\ \text{for heated regions}\\
&\qquad\ \frac{\partial T}{\partial R}=\frac{\partial C}{\partial R}=0, \qquad\qquad \text{for unheated regions}\\
&X=L: \quad P=0.
\end{aligned}$$

Thus the dimensionless parameters for the double-diffusive convection in an open-ended cylindrical annular cavity are

$Pr = \frac{\nu}{\alpha}$, the Prandtl Number, $Gr_T = \frac{g\beta_T \Delta\theta D_h^4}{l\nu^2}$, thermal Grashof Number,

$Sc = \frac{\nu}{D}$, the Schmidt Number, $Gr_M = \frac{g\beta_S \Delta S D_h^4}{l\nu^2}$, solutal Grashof Number,

$N = \frac{\beta_C \Delta S}{\beta_T \Delta\theta}$, Buoyancy ratio, $E = \frac{L_1}{L_2}$, Length ratio,

$\lambda = \frac{r_i}{r_o}$, Radii ratio, $Q = \frac{q}{\pi l Gr\nu}$, Dimensionless volumetric flow rate.

Knowing the temperature and concentration distribution from the numerical solution of energy and species equations, the local Nusselt and Sherwood numbers, a major parameter of practical interest in the study of convective heat and mass transfer at any cross section may be calculated.

The dimensionless form of the heat transfer coefficient is the Nusselt number denoted by and is defined as, in dimensionless form,

$$Nu = \frac{hD_h}{k} = -\frac{\partial T}{\partial R}\Big|_{\text{wall}}.$$

The average Nusselt number $\overline{Nu}$ over the channel length is given by

$$\overline{Nu} = \frac{\int_{L-L_1-L_2}^{L-L_1} NudX}{\int_{L-L_1-L_2}^{L-L_1} dX} = \frac{1}{L_2}\int_{L-L_1-L_2}^{L-L_1} NudX.$$

Similarly, the average Sherwood number $\overline{Sh}$ over the channel length is given by

$$\overline{Sh} = \frac{1}{L_2}\int_{L-L_1-L_2}^{L-L_1} ShdX,$$

where Sh is the local Sherwood number defined as

$$Sh = -\frac{\partial C}{\partial R}\Big|_{\text{wall}}.$$

3 Numerical procedure

Since the governing partial differential equations are non linear and coupled, a general analytical solution is not possible. Hence the set of coupled governing equations, subject to the boundary conditions, are numerically solved by a fully implicit finite difference scheme. The implicit finite difference technique, used in this paper, has been previously used by many authors for both parallel plates and annular geometries with

great success (Coney and El-Shaarawi [2], El-Shaarawi and Sarhan [3], Yan and Lin [6] and Bodia and Osterle [7]). Because of the flow under consideration is a boundary layer type, the solution of the Eqs. (2.5a)-(2.5d) can be marched in the downstream direction. In the implicit numerical scheme, used here, the derivatives in the axial direction are approximated by backward difference, due to marching the solution in downstream direction, and the derivatives in the radial direction are approximated by central difference. The implementation of the scheme to the governing equations is briefly given below.

3.1 Implementation to continuity equation

Replacing the derivatives in Eq. (2.5a) by the following finite difference approximations

$$\frac{\partial U}{\partial R}\Big|_{i+\frac{1}{2},j+1} = \frac{U_{i+1,j+1}-U_{i,j+1}}{\Delta R} \qquad \text{(central difference)},$$

$$\frac{\partial W}{\partial X}\Big|_{i+\frac{1}{2},j+1} = \frac{W_{i+\frac{1}{2},j+1}-W_{i+\frac{1}{2},j}}{\Delta X} \qquad \text{(backward difference)},$$

and putting

$$W_{i+\frac{1}{2},j+1} = \frac{W_{i+1,j+1}+W_{i,j+1}}{2}, \qquad W_{i+\frac{1}{2},j} = \frac{W_{i+1,j}+W_{i,j}}{2},$$

$$\frac{U}{R}\Big|_{i+\frac{1}{2},j+1} = \frac{U_{i+1,j+1}+U_{i,j+1}}{2\Big[\lambda^{-1}+\big(i-\frac{1}{2}\big)\Delta R\Big]}.$$

Eq. (2.5a) in finite difference form read as:

$$\frac{U_{i+1,j+1}+U_{i,j+1}-U_{i,j}}{2\Delta R}+\frac{W_{i+1,j+1}-W_{i,j+1}}{\Delta X}+\frac{U_{i+1,j+1}+U_{i,j+1}}{2\Big[\lambda^{-1}+\big(i-\frac{1}{2}\big)\Delta R\Big]}=0,$$

or

$$U_{i+1,j+1} = A_1 U_{i,j+1} - B_1(W_{i+1,j+1}+W_{i,j+1}-W_{i+1,j}-W_{i+1,j}-W_{i,j}),$$

for $i = 1, \cdots, I\max-2$, for each $j = 1, \cdots, J\max$, where

$$A_1 = \frac{\lambda^{-1}+(i-1)\times\Delta R}{\lambda^{-1}+i\times\Delta R},$$

$$B_1 = \Big(\frac{\Delta R}{4\Delta X}\Big)\Big[\frac{2\lambda^{-1}+(2i-1)\times\Delta R}{\lambda^{-1}+i\times\Delta R}\Big].$$

3.2 Implementation to axial momentum equation

The derivatives in Eq. (2.5b) are replaced by the following finite difference approximations

$$\frac{\partial W}{\partial R}\Big|_{i,j+1} = \frac{W_{i+1,j+1} - W_{i-1,j+1}}{2\Delta R} \quad \text{(backward difference)},$$
$$\frac{\partial W}{\partial X}\Big|_{i,j+1} = \frac{W_{i,j+1} - W_{i,j}}{\Delta X} \quad \text{(backward difference)},$$
$$\frac{\partial P}{\partial X}\Big|_{i,j+1} = \frac{P_{i,j+1} - P_{i,j}}{\Delta X} \quad \text{(backward difference)},$$
$$\frac{\partial^2 W}{\partial R^2}\Big|_{i,j+1} = \frac{W_{i+1,j+1} - 2W_{i,j+1} + W_{i-1,j+1}}{(\Delta R)^2} \quad \text{(central difference)}.$$

Using the above approximations, Eq. (2.5b) in finite difference form becomes

$$A_2 W_{i-1,j+1} + B_2 W_{i,j+1} + C_2 W_{i+1,j+1} + E_2 P_{i,j+1} = D_2(i-1),$$

for $i = 2, \cdots, I\max - 1$, for each $j = 1, 2, \cdots, J\max$, where,

$$A_2 = \frac{1}{\lambda^{-1} + (i-1)\times\Delta R} - \frac{U_{i,j}}{2\Delta R} - \frac{1}{(\Delta R)^2}, \qquad B_2 = \frac{W_{i,j}}{\Delta X} + \frac{2}{(\Delta R)^2},$$
$$C_2 = \frac{U_{i,j}}{2\Delta R} - \frac{1}{\lambda^{-1} + (i-1)\times\Delta R} + \frac{1}{(\Delta R)^2}, \qquad E_2 = \frac{1}{\Delta R},$$
$$D_2 = \frac{W_{i,j}^2}{\Delta X} + \frac{P_{i,j}}{\Delta X} - \frac{(T_{i,j+1} + N\times C_{i,j+1})}{16(1-\lambda)^4}.$$

3.3 Implementation to energy equation

Using the following finite difference approximations

$$\frac{\partial T}{\partial R}\Big|_{i,j+1} = \frac{T_{i+1,j+1} - T_{i-1,j+1}}{2\Delta R},$$
$$\frac{\partial T}{\partial X}\Big|_{i,j+1} = \frac{T_{i,j+1} - T_{i,j}}{\Delta X},$$
$$\frac{\partial^2 T}{\partial R^2}\Big|_{i,j+1} = \frac{T_{i+1,j+1} - 2T_{i,j+1} + T_{i-1,j+1}}{(\Delta R)^2},$$

the energy equation (2.5c) in finite difference form is

$$A_3 T_{i-1,j+1} + B_3 T_{i,j+1} + C_3 T_{i+1,j+1} = D_3(i-1).$$

Here, for $i = 2, \cdots, I\max - 1$, for each $j = 1, 2, \cdots, J\max$ (for UWT) and for $i = 1, 2, \cdots, I\max$, for each $j = 1, 2, \cdots, J\max$ (for UHF), where

$$A_3 = \frac{1}{2\left[\lambda^{-1} + (i-1)\times\Delta R\right]\Pr\Delta R} - \frac{U_{i,j}}{2\Delta R} - \frac{1}{\Pr(\Delta R)^2}, \qquad B_3 = \frac{W_{i,j}}{\Delta X} + \frac{2}{\Pr(\Delta R)^2},$$
$$C_3 = \frac{U_{i,j}}{2\Delta R} - \frac{1}{2\left[\lambda^{-1} + (i-1)\times\Delta R\right]\Pr\Delta R} - \frac{1}{\Pr(\Delta R)^2}, \qquad D_3 = \frac{W_{i,j}T_{i,j}}{\Delta X}.$$

In a similar way, the concentration equation can also be written in terms of finite difference equation and is not repeated here for the brevity of the manuscript. Finally, the integral continuity Eq. (2.5e) can be written, using Simpson's rule, in the following form:

$$Q = \frac{2\Delta R}{3}\left[4(W_{2,j} + W_{4,j} + W_{6,j} + \cdots) + 2(W_{3,j} + W_{5,j} + W_{7,j} + \cdots)\right].$$

It should be noted that the boundary condition

$$W_{1,j} = W_{I\,\max,j} = 0,$$

is used in the above equation. Bodia and Osterle [7] has shown that the finite difference form of the governing equations are consistent and stable for all mesh ratios. The application of the finite difference equations with appropriate boundary conditions to the present problem is explained as follows.

Using a guess value of the volumetric flow rate or mass flux, Q, at the entrance and applying Eq. (2.5e) we get the inlet velocity W_0 and hence the inlet pressure P_0. For the given value of Q, we apply finite difference form of the energy equation to all the points in the first column (at the channel inlet). The above system of finite difference equations forms a tridiagonal matrix which can be efficiently solved by the Thomas algorithm. After obtaining the values of T, we can compute W and P from the momentum equation. The simultaneous finite difference equations are solved by Gauss elimination scheme. After calculating T, W and P, the values of U are calculated from the finite difference form of the continuity equation. It is important to mention that in the present finite difference technique, the finite difference equations are linearized by assuming that wherever the product of two unknowns occurs, one of them is taken approximately by its value at the previous axial step. Thus the variables with subscript $j+1$ represent the unknowns and those with subscript j are known. Also it is clear that decreasing the axial grid size implies the decrease in the effect of linearization in the finite difference representation of the governing equations. In order to determine a proper grid size for this study, a grid independence test was conducted with different grid sizes. In the present study, 81 grids in the radial direction were used, while the grids in the axial direction range from 501 to 801, depending on the Grashof number and the length of unheated entry, heated section and unheated exit. The values of the average Nusselt number and Sherwood number were used as a sensitivity measure of the accuracy of the solution.

For each value of Q, the above calculation procedure begins at the bottom of the annulus and continues upward until either the pressure becomes zero, which is negative at the inlet, or up to the annulus exit. It should be remembered that the inlet velocity W_0 is not known a priori. In fact, it depends in a complicated way upon the thermal and hydrodynamic conditions imposed on the system and the same will be determined by the iterative procedure in the solution process. Thus we take two guess values of Q such that the product of pressure at the annulus exit is negative for these values of Q. Then the bisection method is used to obtain the exact value of Q for which

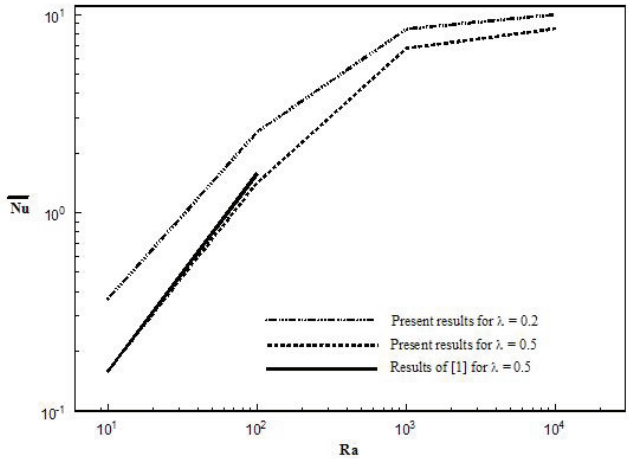

Figure 2: Comparison between the present results and the numerical results of El-Shaarawi and Sarhan [1] for the natural convection ($N = 0$) in an open ended vertical annulus.

the pressure becomes zero at the annulus exit. Further, it is found that for this value of Q, the overall mass fluxes at the top and bottom of the annulus are same and hence the mass conservation principle is satisfied. Then the inlet velocity W_0 is obtained from the value of Q. After obtaining the correct value of Q using Bisection method at the bottom, it is used to in the calculation to obtain the values of temperature, concentration, velocity and pressure at all the downstream locations of the annuli.

The fully developed flow occurs when the annulus height is sufficiently large or when the Rayleigh number is small. The study of fully developed convective flow provides an analytical check on the numerical solution as it yields the limiting conditions for the developing flow. Prior to the calculations, as a partial verification of the computational procedure for the present problem, the numerical results for the limiting case of natural convection flows with uniform heating over the full channel length are first obtained. Excellent agreement was found between the present predictions and that of El-Shaarawi and Sarhan [1]. It was found that for small values of Rayleigh number, at which fully developed flow assumption is valid, the present numerical results are in excellent agreement with the results of El-Shaarawi and Sarhan [1].

4 Results and discussion

A numerical study of double diffusive natural convection heat transfer in an open-ended vertical cylindrical annulus has been made to understand the effect of discrete heating boundary condition. In this study both the thermal boundary conditions namely, UWT/UWC and UHF/UMF have been considered. In the present study, there are seven dimensionless groups namely, Prandtl number, Pr, Grashof numbers due to temperature and concentration, Gr_T, Gr_M, Schmidt number, Sc, buoyancy ratio, N, length ratio (the ratio between heated and unheated section) E, and the radii ratio λ,

which is an important parameter in cylindrical annular geometry. The computations were performed for the following range of physical parameters of the problem. The thermal Grashof number, Prandtl number and Schmidt number are fixed respectively at 10^4, 0.7 and 0.2. The buoyancy ratio is varied from 0.1 to 2, radii ratio from $\lambda = 0.1$-0.9. The length ratio is chosen to have the values from 0.5-2. This set of values reveals the effect of discrete heating when the heated length is less than, equal to and greater than the unheated length (entry or exit). The results are presented in the form of axial and radial velocity profiles, temperature and concentration profiles and pressure variation with height. The overall rate of heat and mass transfer from the side walls is obtained by evaluating the average Nusselt and Sherwood numbers.

4.1 UWT/UWC

The effect of discrete heating length ratio E on the development of axial, radial velocity profiles and temperature, concentration profiles at different heights of the annulus are shown in Fig. 3 for the values of $N = 0.1$ and $\lambda = 0.1$. From the figure, it can be observed that, near the inlet, radial velocity component transfer the fluid from the boundary to the core of the annulus with high magnitude. As the length ratio increases, the radial velocity undergoes a drastic change. From the axial velocity profiles, it can be clearly seen that the velocity profiles develop gradually from uniform distribution at the inlet to the parabolic one in the fully developed region. For large length ratio ($E = 2$), the fluid moves with higher magnitude. The temperature profile suggests the existence of more gradients for unit length ratio.

Since the heated and unheated lengths are same, for $E = 1$, more gradients are expected near the exit. However, for $E = 0.5$ and $E = 2$, the concentration profiles are nearly flat at the exit due to insulated or unheated exit length. The variation of concentration profiles can be seen only near the heated region. The concentration at the wall is unity due to boundary condition, which decreases with radial distance and then increases near the middle of the annulus to wall concentration. The effect of buoyancy ratio, an important parameter in double diffusive convection, on the velocity, temperature and concentration profiles are depicted in Fig. 4 for $\lambda = 0.9$ and $E = 2$. From the profiles, it is interesting to note that more gradients are found for $N = 2$ due to the combined buoyancy effect. The pattern of velocity profiles remains same for all the values of N. However, a significant variation can be found from the concentration profiles. Also, it is interesting to observe that the temperature decreases faster from the boundary to the core of the annulus as the buoyancy ratio increases.

The influence of radii ratio on the radial velocity and temperature profiles are illustrated in Fig. 5 for $N = 0.1$ and $E = 2$. For $\lambda = 0.1$, the radial velocity component transfers fluid from inner wall of the annulus to outer wall of the annulus, whereas for $\lambda = 0.9$ it mainly transfers fluid from the regions close to the two boundaries to the core fluid. The same phenomenon may also be observed from the developing temperature profiles. The variation of local Nusselt and Sherwood numbers with the dimensionless axial distance X for different length ratios are shown in Fig. 8 for

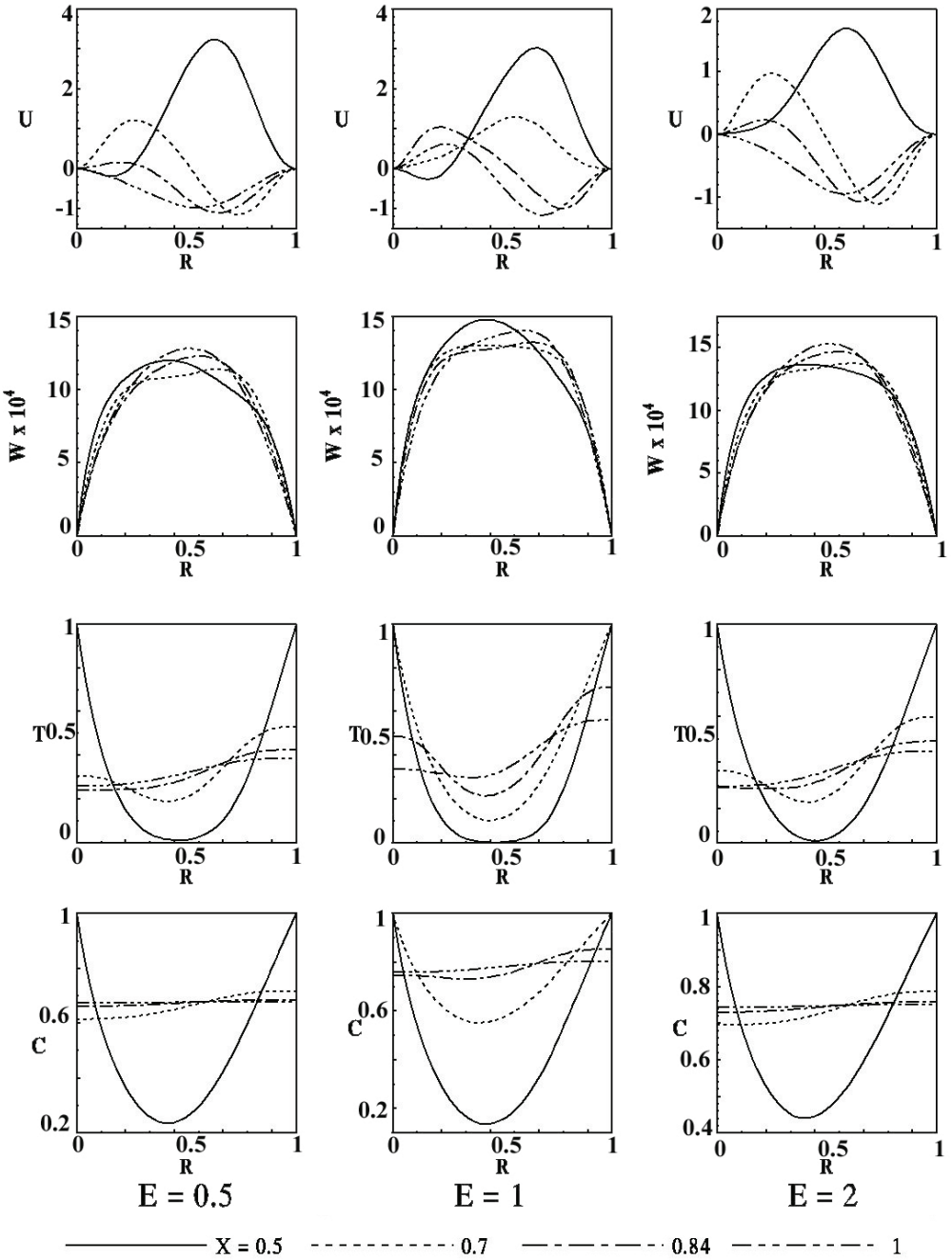

Figure 3: Effect of discrete heating on the development of velocity, temperature and concentration profiles for $N = 0.1$ and $\lambda = 0.1$ for UWT/UWC.

$N = 0.1$ and $\lambda = 0.1$. The Nusselt or Sherwood number, which attains its maximum value at the inlet decreases uniformly to reach a minimum and then reaches constant value. It can also be seen that the rate of heat transfer is found to be more than the

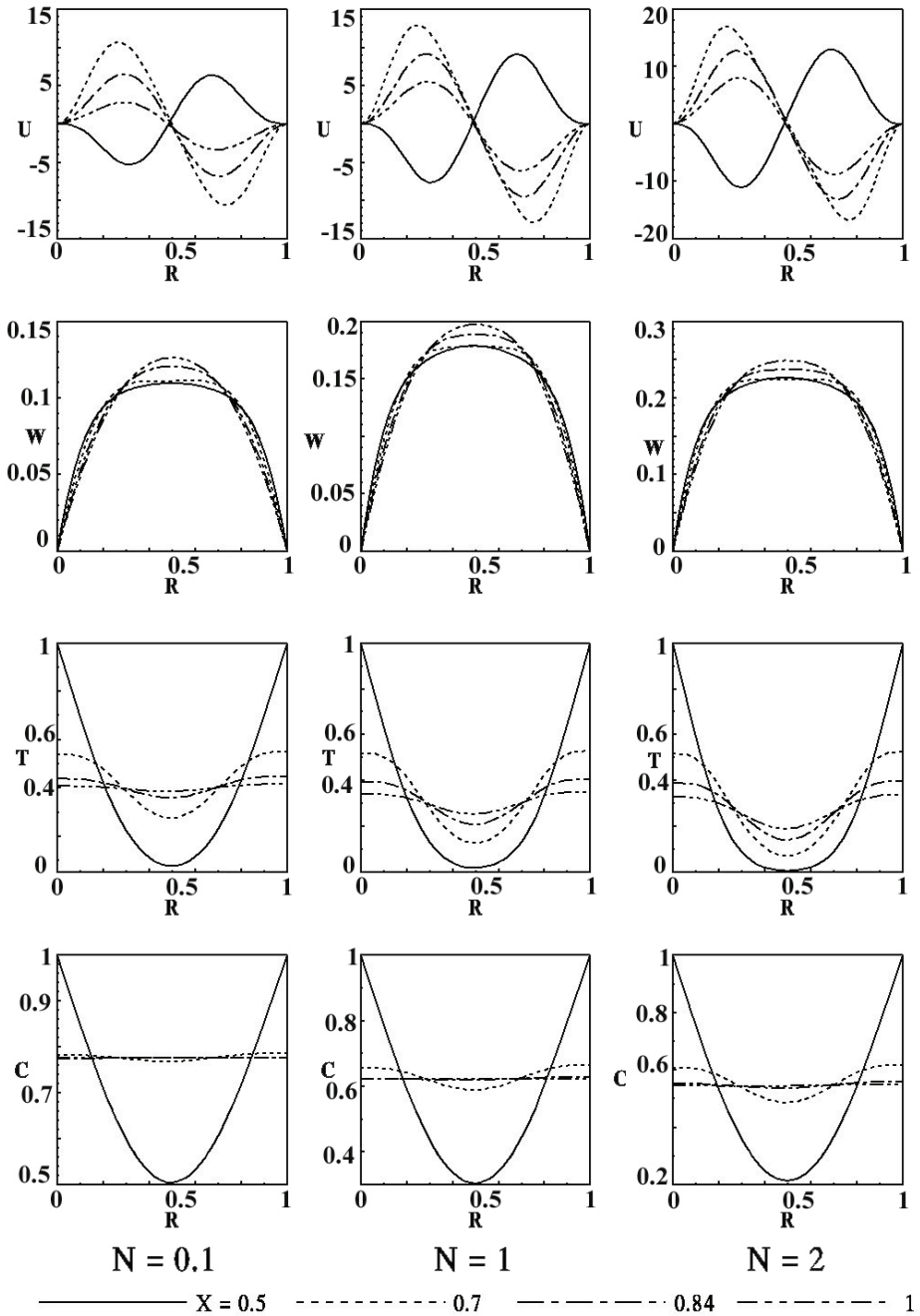

Figure 4: Effect of buoyancy ratio on the development of velocity, temperature and concentration profiles for $\lambda = 0.9$ and $E = 2$ for UWT/UWC.

mass transfer. The effect of radii ratio on the local heat and mass transfer are obtained and is given in Fig. 9 for $N = 0$ and $E = 1$. It is clear from this figure that local Nu and Sh for smaller radii ratio are greater at the same dimensionless axial distance, except

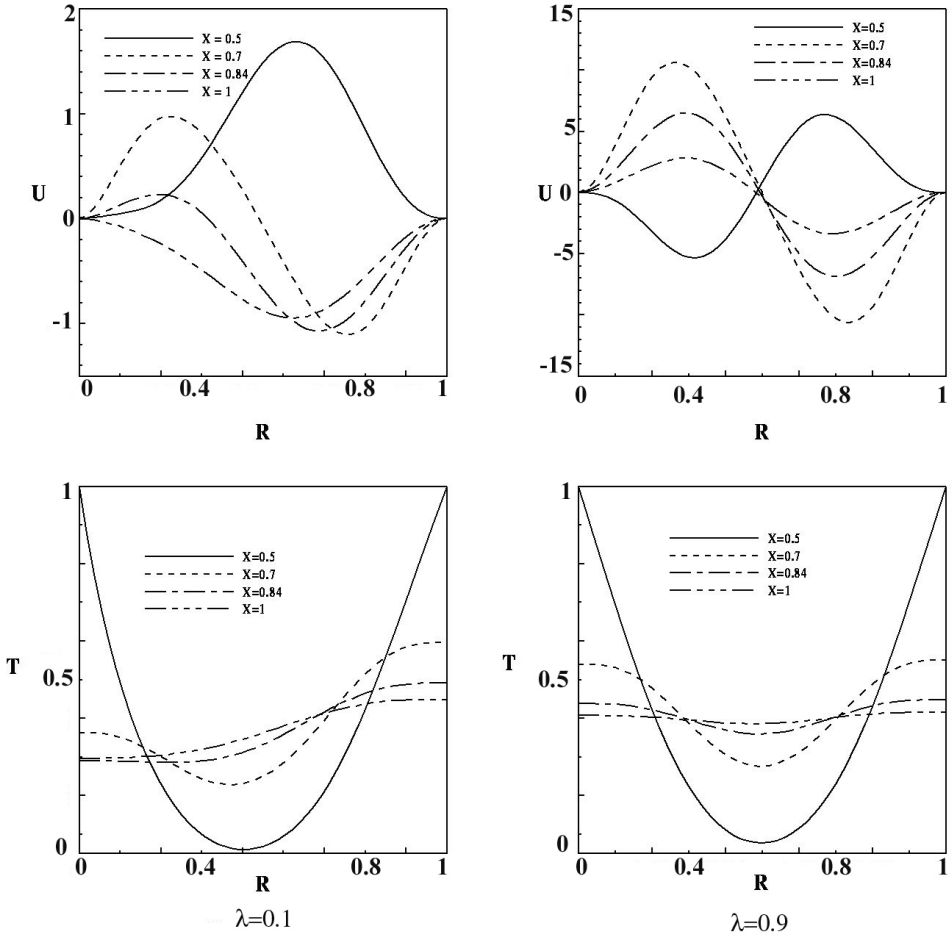

Figure 5: Effect of radii ratio on velocity and temperature profiles for UWT/UWC.

near the entrance, than for the other radii ratios. This phenomenon is further reflected in the variation of pressure defect with the dimensionless axial distance in Fig. 10 for two different values of λ.

4.2 UHF/UMF

The effect of discrete heating condition on velocity, temperature and concentration profiles for $N = 0.1$ and $\lambda = 0.1$ is shown in Fig. 6. The radial velocity profiles had undergone a drastic change when a heat/mass flux is imposed on the side walls of the annulus. The radial velocity components are higher in magnitude compared to UWT/UWC case and transfers the fluid from the boundary to the core. The axial velocity is more pronounced towards outer wall as the fluid moves upwards. The variation of temperature is more vigorous in the middle of the annulus for $E = 1$. As expected, the concentration profiles near the exit are flat. The effect of buoyancy

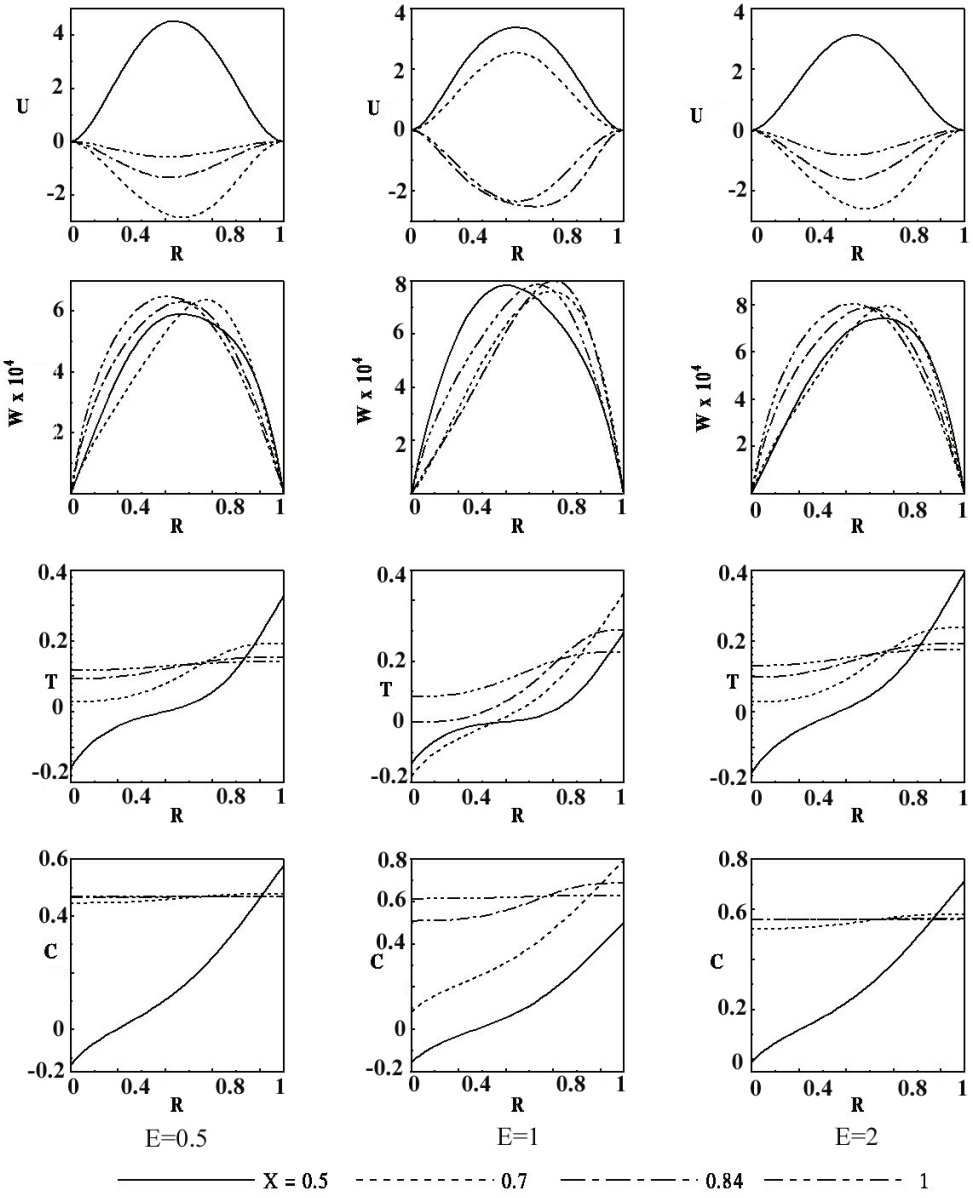

Figure 6: Effect of discrete heating on the development of velocity, temperature and concentration profiles for $\lambda = 0.1$ and $N = 0.1$ for UWT/UWC.

ratio on the velocity, temperature and concentration profiles are shown in Fig. 7 for $\lambda = 0.9$ and $E = 2$. For large buoyancy ratio, the velocity profile suggests that the fluid is moving with larger magnitude than the UWT/UWC case. More temperature and concentration gradients are found in the middle of the annulus. The variation of local Nusselt and Sherwood numbers for different length ratios are given in Fig. 8. Careful inspection discloses that the value of local Nu or Sh, at a given axial distance,

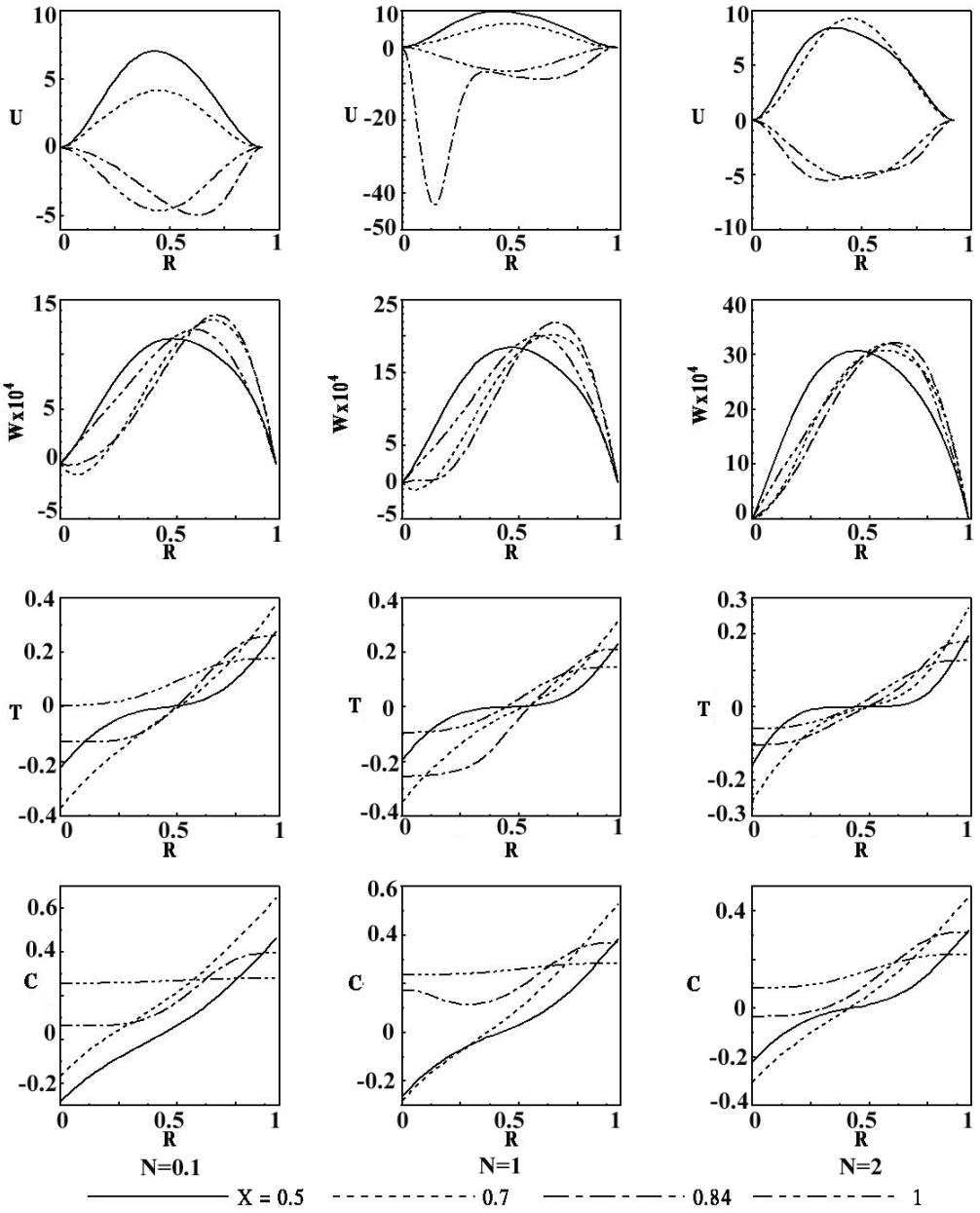

Figure 7: Development of velocity, temperature and concentration profiles for different values of N for UHF/UMF.

is less than the value of Nu or Sh for the UWT/UWC case. The variations of pressure defect for different heating conditions are given in Fig. 10. Initially, the magnitude of pressure defect increases and reaches the value zero to satisfy the boundary condition. It can be observed from the figure that the pressure defect for $E = 1$ is more than that of the other cases of discrete heating. This suggests that this kind of configuration is

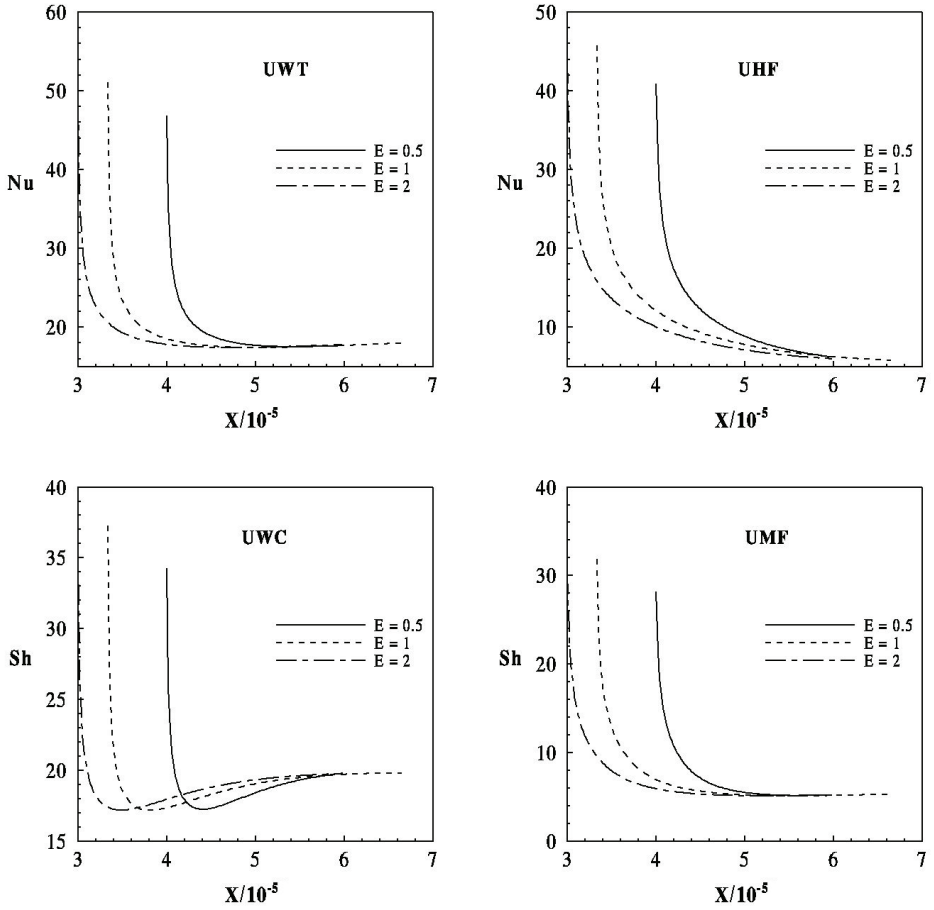

Figure 8: Variation of Nusselt and Sherwood numbers for different length ratios and $N = 0.1$, $\lambda = 0.1$.

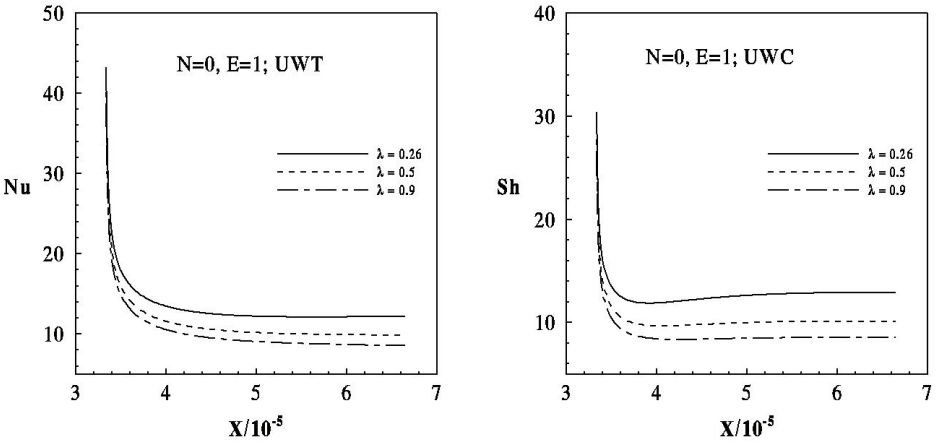

Figure 9: Effect of radii ratio on Nusselt and Sherwood numbers.

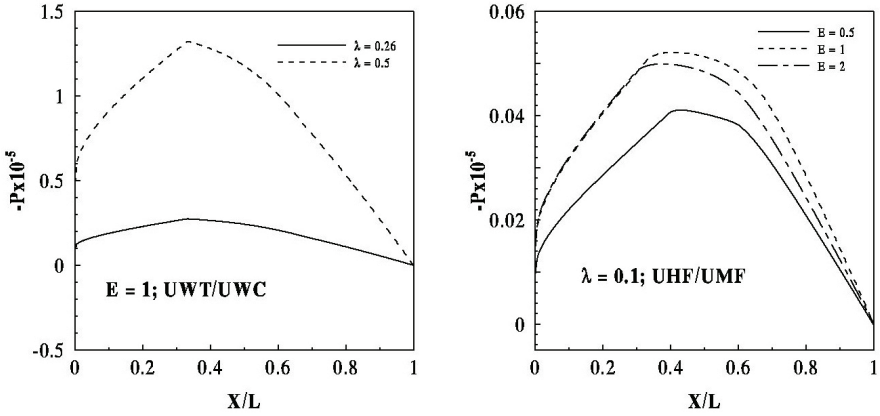

Figure 10: Variation of pressure for different values of λ and E.

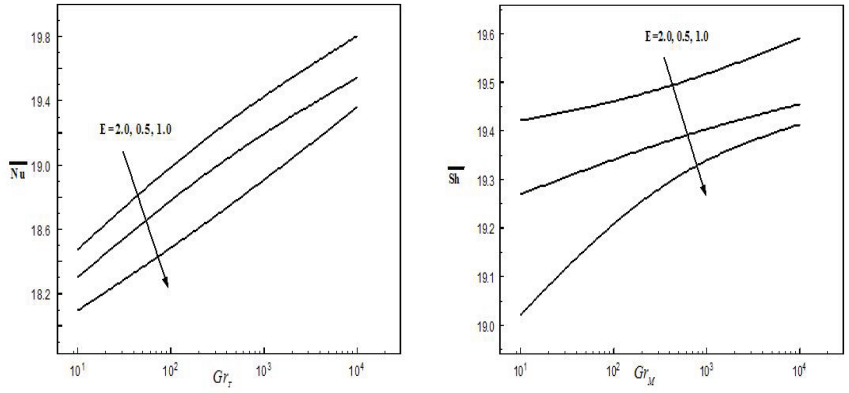

Figure 11: Effect of length ratio on average Nusselt and Sherwood numbers.

more useful for inducing the flow. Fig. 11 illustrates the effect of length ratio on the average heat and mass transfer rates in the annulus. It can be clearly seen from the figure that the heat and mass transfer rates are enhanced with the length ratio.

5 Conclusions

Double diffusive natural convection heat and mass transfer in vertical open-ended cylindrical annulus has been studied numerically. The effect of discrete boundary conditions on the various aspects of heat and mass transfer characteristics have been investigated in detail for a wide range of physical parameters of the problem. The following is the major summary of results:

1. Average Nusselt and Sherwood numbers which describes the heat and mass transfer from the wall to the air is found to be better for $E = 2$,

2. Local Nusselt and Sherwood number is increasing as the radii ratio is decreased,

3. Local heat and mass transfer rates are found to be higher for the UWT/UWC case than that of UHF/UMF,

4. The length ratio $E = 1$ is more useful for inducing the flow,

5. For larger buoyancy ratio, the flow is found to be stronger due to the dominant effect of compositional buoyancy force.

Acknowledgements

The author is grateful to the Chairman and Principal of East Point College of Engineering and Technology, Bangalore for their constant encouragement and support. Also, the author would like to thank Prof. P. Nithiarasu and the anonymous referees for their valuable comments and suggestions to improve the quality of the manuscript.

References

[1] M. A. I. EL-SHAARAWI AND A. SARHAN, *Developing laminar free convection in a heated vertical open-ended concentric annulus*, Ind. Eng. Chem. Fundam., 20 (1981), pp. 388–394.

[2] J. E. R. CONEY AND M. A. I. EL-SHAARAWI, *Finite difference analysis for laminar flow heat transfer in concentric annuli with simultaneously developing hydrodynamic and thermal boundary layers*, Int. J. Numer. Methods. Engg., 9 (1975), pp. 17–38.

[3] M. A. I. EL-SHAARAWI AND A. SARHAN, *Developing laminar free convection in an open ended vertical annulus with a rotating inner cylinder*, ASME. J. Heat. Trans., 103 (1981), pp. 552–558.

[4] K. HASHIMOTIO, N. AKINO AND H. KAWAMURA, *Combined forced-free laminar heat transfer to a highly heated gas in a vertical annulus*, Int. J. Heat. Mass. Trans., 29(1) (1986), pp. 145–151.

[5] M. A. AL-NIMAR, *Analytical solution for transient laminar fully developed free convection in vertical concentric annuli*, Int. J. Heat. Mass. Trans., 36(9) (1993), pp. 2385–2395.

[6] W. M. YAN AND D. LIN, *Natural convection heat and mass transfer in vertical annuli with film evaporation and condensation*, Int. J. Heat. Mass. Trans., 44 (2001), pp. 1143–1151.

[7] J. R. BODIA AND J. F. OSTERLE, *The development of free convection between heated vertical plates*, ASME. J. Heat. Trans., 84 (1962), pp. 40–44.

[8] W. M. YAN AND T. F. LIN, *Natural convection heat transfer in vertical open channel flows with discrete heating*, Int. Comm. Heat. Mass. Trans., 14 (1987), pp. 187–200.

[9] K. T. LEE, *Natural convection in vertical parallel plates with an unheated entry or unheated exit*, Numer. Heat. Trans. A., 25 (1994), pp. 477–493.

[10] D. J. NELSON AND B. D. WOOD, *Combined heat and mass transfer natural convection between vertical parallel plates with uniform flux boundary conditions*, Int. J. Heat. Mass. Trans., 4 (1986), pp. 1587–1592.

[11] T. S. CHEN AND C. F. YEH, *Combined heat and mass transfer in natural convection along a vertical cylinder*, Int. J. Heat. Mass. Trans., 23 (1980), pp. 451–461.

[12] K. T. LEE, *Natural convection heat and mass transfer in partially heated vertical parallel plates*, Int. J. Heat. Mass. Trans., 42 (1999), pp. 4417–4425.

[13] K. T. LEE, *Fully developed laminar natural convection heat and mass transfer in partially heated vertical pipe*, Int. Commun. Heat. Mass. Trans., 27(7) (2000), pp. 995–1001.

[14] C. Y. CHENG, *Fully developed natural convection heat and mass transfer in a vertical annular porous medium with asymmetric wall temperature and concentrations*, Appl. Therm. Engg., 26 (2006), pp. 2442–2447.
[15] H. A. MOHAMMED AND Y. K. SALMAN, *Heat transfer by natural convection from a uniformly heated vertical circular pipe with different entry restriction configurations*, Energ. Convers. Manage., 48(7) (2007), pp. 2244–2253.
[16] R. W. LEWIS, P. NITHIARASU AND K. N. SEETHARAMU, Fundamentals of the Finite Element Method for Heat and Fluid Flow, Wiley, 2004.